

# Definition of an optimal solutioning treatment for a Ni-based superalloy processed by Additive Manufacturing

P.A. Martelli, M.S. Kenevisi, E. Bassini, D. Ugues

The current work aims at defining an optimal recipe for the solution annealing (SA) of a high-fraction  $\gamma'$  Ni-based superalloy manufactured with Laser Powder Bed Fusion process (PBF-LB/M). The studied alloy is designed for the aeronautical or energy sectors to perform above 800°C. The microstructure obtained from PBF-LB/M process (as-built state) is extremely fine with grains aligned along the building direction, due to the thermal flow during the process. Moreover, due to the fast cooling, the main reinforcing phase ( $\gamma'$ , a  $\text{Ni}_3(\text{Al,Ti})$  ordered  $\text{L1}_2$  precipitate) cannot precipitate. SA temperatures of 1230°C, 1245°C and 1260°C were investigated to obtain the best microstructure in terms of reinforcing precipitates' size, shape and fraction and grain size, keeping the soaking time constant (2 hours). Then, a first aging (FA) was also applied at 1095°C for 4 hours. The test plan was configured to account for industrial furnaces thermal uncertainty, introducing also higher temperatures to verify the presence of any thermal induced porosities (TIPs) or incipient melting traces. The morphology, size and volume fraction of  $\gamma'$  phase were assessed and quantified using scanning electron microscopy (SEM). Light optical microscopy (LOM) was used to evaluate the grains aspect ratio and growth during SA.

**KEYWORDS:** NICKEL SUPERALLOY, HEAT TREATMENT, ADDITIVE MANUFACTURING, PBF/LB, PRECIPITATION HARDENING, GRAIN COARSENING

## INTRODUCTION

Ni-based superalloys are typically used in high temperature environment such as aeronautics and energy production, due to their outstanding thermo-mechanical properties and resistance to oxidation (1). Among others, René 80 is mainly reinforced by precipitation hardening of  $\text{L1}_2$  ordered  $\text{Ni}_3(\text{Al,Ti})$  phase  $\gamma'$  in a face-centered cubic (FCC) matrix  $\gamma$ . René 80 is traditionally processed by investment casting (2), but additive manufacturing techniques are gaining interest due to the capability to produce complex near-net shape components. In particular, Laser Powder Bed Fusion (PBF-LB) has already given promising results in terms of densification of such alloy (3). However, a peculiar microstructure is originated after the rapid heating-cooling cycles of PBF-LB process. More specifically, René 80 shows a cellular structure within fine grains elongated along the building direction (3). To optimize the as-built microstructure, solution annealing (SA) and aging treatments are necessary to guarantee the optimal shape, fraction and size of the reinforcing  $\gamma'$  precipitates as well as grains' recrystallization and coarsening (4). When it comes to additive manufacturing, the complex and new

**P. A. Martelli, M. S. Kenevisi**

Politecnico di Torino and Centro Interdipartimentale  
Integrated Additive Manufacturing, Italy

**E. Bassini, D. Ugues**

Politecnico di Torino, Centro Interdipartimentale Integrated  
Additive Manufacturing and Consorzio  
Nazionale della Scienza e Tecnologia dei Materiali, Italy

microstructure originated from the printing stage requires different treatment conditions with respect to the traditional processes, after which SA is typically performed at 1204°C (5,6). For this reason, the commonly adopted annealing temperatures should be changed accordingly. The aim of the present work is to provide an optimized SA + first aging (FA) recipe, demonstrating that older heat treatments are less effective when applied to additively manufactured materials. Optimized process parameters (3) were used to process René 80 powders and different temperatures were studied to find the  $\gamma'$  solvus temperature and the optimal SA condition in terms of precipitates' size, morphology and fraction using scanning electron microscopy (SEM). Grains' recrystallization and growth process was also assessed using light optical microscopy (LOM). FA was

performed at 1095°C for 4 hours. The results demonstrated that the SA temperature shall be set at 1260°C to achieve the full dissolution of  $\gamma'$  and grains' recrystallization. Given the typical thermal variability of industrial furnaces, one sample was also treated raising the SA to 1270°C to assess possible thermal induced porosities (TIP) formation or incipient melting.

## MATERIALS AND METHODS

### Material and samples production

The raw material used for producing the samples is a gas atomized powder commercialised as Ni-183 by Praxair Inc. The nominal composition of René 80 is reported in Tab. 1. The powders were sieved by the manufacturer in the range of 16 to 45 $\mu$ m.

**Tab.1** - Nominal chemical composition for René 80 powders.

RENÉ 80 POWDERS NOMINAL CHEMICAL COMPOSITION (%WT)							
Cr	Co	Mo	W	Al	Ti	Zr	Ni
13.5-14.5	7.5-12.5	3.5-4.5	3.5-4.5	2.5-3.5	4.5-5.5	0.02-0.1	Bal.

Cubic samples of 20mm of edge were produced using a PrintSharp250 system by Prima Additive with a 250x250mm carbon steel platform heated to 80°C and a rubber recoater.

Printing parameters were optimised by the authors in a previous work (3) and are summarized in Tab. 2. Each stripe of the scanning was rotated of 67° between each layer.

**Tab.2** - Optimization range for the main printing parameters.

Main parameters optimization range		
Laser Power (W)	Scan Speed (mm/s)	Hatching Distance (mm)
170-195	1000-1900	0.03-0.08

### Post processing

Samples were cut from the building platform using Wire Electro Discharge Machining (WEDM) and they underwent a stress relief treatment at 1080°C for 2 hours. After this step, solution annealing (SA) and first aging (FA) were applied in a low-pressure furnace TAV mini jet. The SA was carried out at 1230°C, 1245°C and 1260°C for 2 hours, then gas cooling with nitrogen at about 100°C/min was applied to reach the first aging temperature (1095°C), which was maintained for 4 hours. Finally, another sample underwent SA at 1270°C for 2h + FA to assess the risk of thermal induced porosities (TIPs) formation and incipient melting.

### Samples preparation and investigation

Samples were metallography prepared along the building direction (XZ plane). Sections were embedded in resin and ground with SiC papers up to 1200 grit and polished with diamond suspensions of 6-3-1 $\mu$ m. Colloidal silica of 0.04 $\mu$ m was used to reach the final surface finishing. The  $\gamma'$  morphology was assessed using a Zeiss EVO15 Scanning Electron Microscope (SEM) after electrolytic etching with H<sub>3</sub>PO<sub>4</sub> (30%vol. in distilled water) at 3.5V. Chemical etching with Kalling n°2 solution was used to measure size and volume fraction of secondary  $\gamma'$ ; for this purpose, six back-scattered electron images at 10.00kX were analysed with an ImageJ algorithm developed by the authors. Grain size was

measured both along (Z-dir) and across (X-dir) building direction using the linear intercept method (ASTM E112-13) on three images at 100X taken with a Leica DZ500 light optical microscope (LOM).

### Hardness test

Brinell hardness tests were performed according to ASTM E10-18 with a force of 62.5 kg (HB10) on each sample, with 3 repetitions on the XZ plane, using a EMCOTEST M4U 025 system.

## RESULTS

### Microstructure evolution after solution annealing and first aging treatments

Fig. 1 shows the microstructure after the SA performed at different temperatures ranging from 1230°C to 1260°C. The electrolytic etching dissolved the  $\gamma$  matrix (yellow arrow), making the precipitates (black arrow) clearly visible.

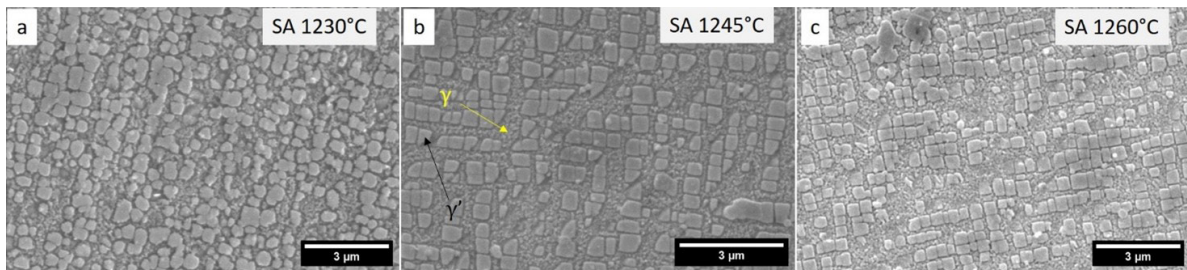


**Fig. 1** - Detail of  $\gamma'$  precipitates after SA at b) 1230°C, c) 1245°C and d) 1260°C for 2 hours and subsequent FA at 1095°C for 4 hours. Yellow and black arrow indicate  $\gamma$  and  $\gamma'$ , respectively.

After SA at 1230°C,  $\gamma'$  is still irregular in shape. On the other hand, when the SA temperature is increased up to 1245°C and 1260°C, precipitates become cubic and regularly arranged. Back-scattered electron images were used to assess the size of  $\gamma'$  precipitates and results are shown in Fig. 2. The mean size of  $\gamma'$  remained quite constant and was calculated to be 239±114nm annealing at 1230°C, 283±133nm at 1245°C and 264±109nm at 1260°C. A similar result was obtained for the  $\gamma'$  fraction, which was 20.4±0.5%, 22.3±1.1% and 21.4±4.2% after SA at

1230°C, 1245°C and 1260°C, respectively. The results can be considered independent from the SA temperature, considering the measure uncertainty. The main difference between the treatment conditions lays in the morphology of secondary  $\gamma'$ . The results show that at 1230°C the proper SA temperature is not reached, while starting from 1245°C the  $\gamma'$  dissolution is effective and the further precipitation and aging lead to precipitates having a regular cuboidal shape.

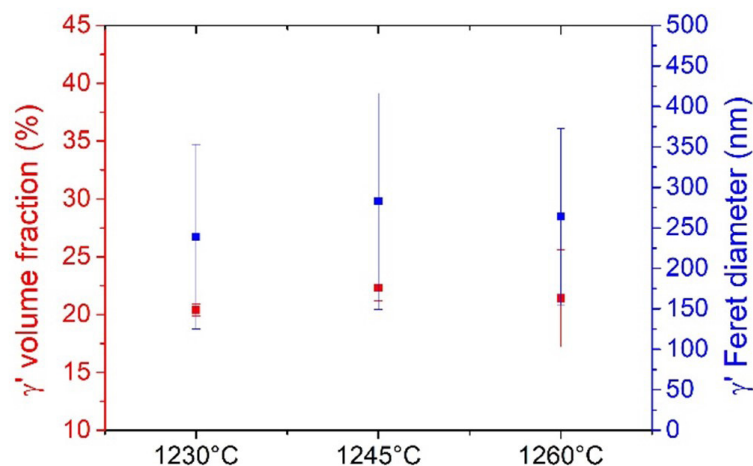


**Fig. 2** - Fraction (%) and size (nm) of the secondary  $\gamma'$  in solution annealed + aged René 80 alloy.

The different SA treatments also led to different grain structures (Fig. 3). The sample treated at 1230°C still shows thin and elongated grains due to the additive manufacturing process (Fig. 3a), which demonstrates that the applied temperature was insufficient to promote a complete recrystallization. Traces of recrystallization can be observed when the SA is performed at 1245°C. More

specifically, larger grains with an aspect ratio closer to unity can be seen (Fig. 3b). In particular, small areas with equiaxial grains can be detected (red circle). Finally, SA at 1260°C led to a fully recrystallized structure (Fig. 3c), which is testified by the diffuse presence of equiaxial grains.

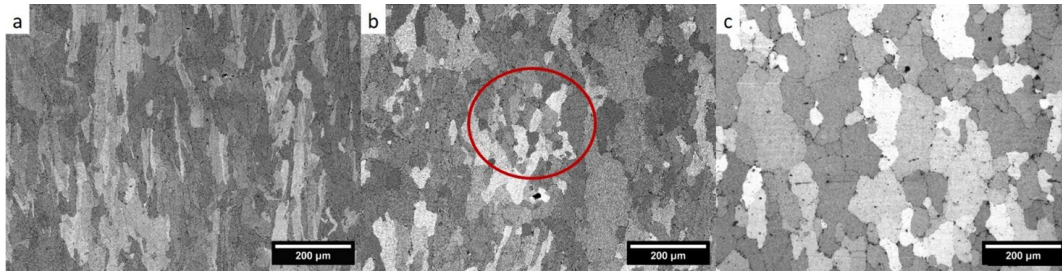


**Fig. 3** - Grains observed under LOM after SA at a) 1230°C, b) 1245°C and c) 1260°C

Grain size was assessed and the values are reported in Fig. 4a. Increasing the SA temperature, the grain size measured along the X direction (perpendicular to the building direction) increases from  $15.3 \pm 0.4 \mu\text{m}$  at 1230°C to  $28.9 \pm 3.2 \mu\text{m}$  and  $45.8 \pm 5.7 \mu\text{m}$  at 1245°C and 1260°C, respectively. Along the building direction (Z) the grain size is similar after SA at 1230°C and 1245°C ( $45.1 \pm 4.6 \mu\text{m}$  and  $43.6 \pm 18.3 \mu\text{m}$ , respectively) and it increases to  $58.1 \pm 9.8 \mu\text{m}$  after SA at 1260°C. The increment in the grain size is consistent with the recrystallization process taking place. In particular, after SA at 1245°C, the process is not fully accomplished and there is only an increase in the mean value measured along the X direction. Instead,

SA performed at 1260°C led to grain coarsening in both the principal directions. Once the recrystallization process takes place, the grains tend to be more equiaxial and this is evidenced by the reduction in the aspect ratio from 3,0 (SA at 1230°C) to 1,5 (SA at 1245°C) and 1,3 (SA at 1260°C). The very high standard deviation measured after SA at 1245°C in the Z-direction is related to the recrystallization areas represented by the red circle in Fig. 3b. The grain coarsening led also to a softening behaviour of the alloy and the Brinell hardness decreased from  $360.0 \pm 7.9$  (SA at 1230°C) to  $345.5 \pm 6.9$  (SA at 1245°C) and  $338.5 \pm 5.9$  (SA at 1260°C), as reported in Fig. 4b.

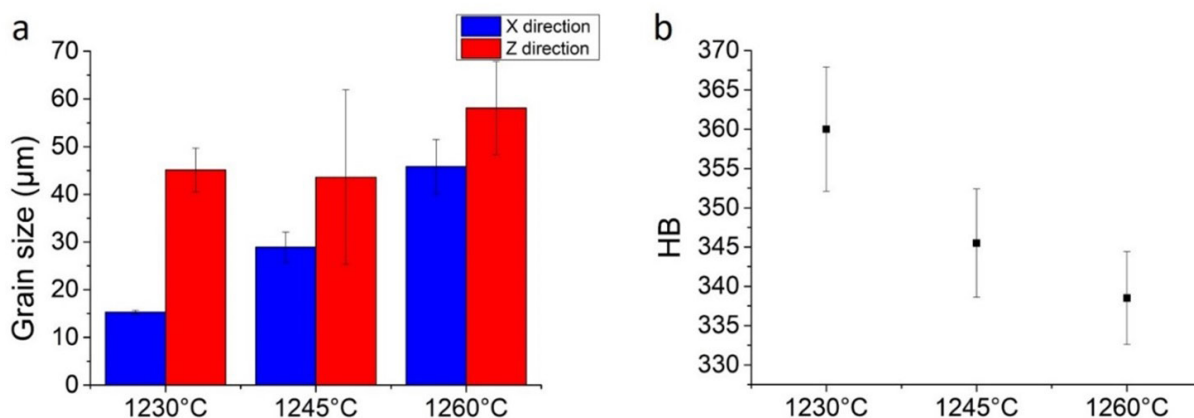


**Fig. 4** - a) Grain size measured along X and Z direction and b) Brinell hardness as a function of SA temperature.

Considering the abovementioned results, 1260°C can be considered as the optimal temperature for SA of PBF-LB René 80 alloy. Given the typical thermal variability of industrial furnaces, a test at 1270°C was also performed to ensure this upper limit does not cause any detrimental consequence in the material, such as TIPs or incipient melting. The sample after SA at 1270°C and FA is showed

in Fig. 5. The secondary  $\gamma'$  is still cubic and its volume fraction and size were assessed to be 23.1+/-2.4% and 344+/-166nm. Beside a slight coarsening of the  $\gamma'$  at grain boundaries, neither evident signs of incipient melting nor thermal induced porosities (TIP) after SA were observed, giving credit to the robustness of the SA performed at 1260°C.

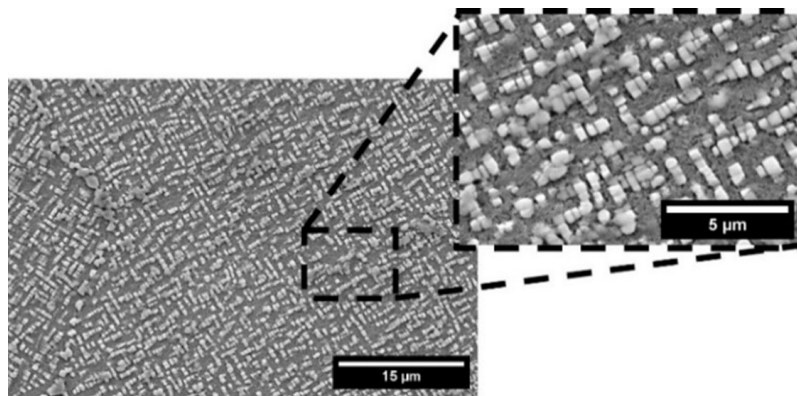


**Fig. 5** -Sample after electrolytic etching treated with SA at 1270°C/2h + FA at 1095°C/4h.

## CONCLUSIONS

In this work René 80 processed with PBF-LB technique was investigated to assess the best heat treatment recipe studying  $\gamma'$  shape, size and fraction and grains' recrystallization. Given a fixed FA condition (1095°C/4h), three different SA temperatures were investigated (1230°C, 1245°C and 1260°C), leading to the following main results:

- The size of  $\gamma'$  was almost constant among the different SA conditions: 239+/-114nm at 1230°C, 283+/-133nm at 1245°C and 264+/-109nm at 1260°C. A similar result was obtained for the  $\gamma'$  volume fraction, which was 20.4+/-0.5%, 22.3+/-1.1% and 21.4+/-4.2% after SA at 1230°C, 1245°C and 1260°C, respectively.
- Reasonably, when a proper  $\gamma'$  dissolution is reached, the nuclei formed after the cooling from the SA grow in the same manner during the FA and the cuboidal shape is obtained. Instead, if the SA temperature is too low, an irregular shape is maintained also during the FA.
- After SA at 1230°C, grains were elongated along the building direction, while SA temperatures of 1245°C and 1260°C progressively led to more equiaxial and recrystallized grains. Grains' aspect ratio decreased from 3,0 (SA at 1230°C) to 1,5 and 1,3 (SA at 1245°C

and 1260°C, respectively).

- Given the abovementioned results, the following recipe for heat treatment of PBF-LB René 80 alloy is proposed: SA at 1260°C for 2 hours + FA at 1095°C for 4 hours. The robustness of the process was investigated heat-treating one sample at 10°C above the optimal SA temperature and neither thermal induced porosities (TIPs) nor incipient melting were observed.

This study provides evidence that the typical heat treatments conditions shall be reconsidered when it comes to AM microstructures. Further studies will focus on assessing the effect of Hot Isostatic Pressing (HIP) on the densification flaws and merging HIP and SA treatment to further optimize the total cycle time.

## ACKNOWLEDGEMENT

This conference communication is part of the project NODES which has received funding from the MUR – M4C2 1.5 of PNRR with grant agreement no. ECS00000036.

**REFERENCES**

- [1] Shirani Bidabadi MH, Yu Z, Rehman A, He JG, Zhang C, Chen H, et al. High-Temperature Oxidation Behavior of CrMoV, F91 and Mar-M247 Superalloys Exposed to Laboratory Air at 550 °C. *Oxid Met* [Internet]. 2018;90(3–4):401–19. Available from: <https://doi.org/10.1007/s11085-018-9839-4>
- [2] Donachie MJ, Donachie SJ. *Superalloys: A technical Guide*. Vol. 36. 2002. 405–479 p.
- [3] Martelli PA, Sivo A, Calignano F, Bassini E, Biamino S, Ugues D. Parameters Optimization and Repeatability Study on Low-Weldable Nickel-Based Superalloy René 80 Processed via Laser Powder–Bed Fusion (L-PBF). *Metals* (Basel). 2023;13.
- [4] Qiu C, Wu X, Mei J, Andrews P, Voice W. Influence of heat treatment on microstructure and tensile behavior of a hot isostatically pressed nickel-based superalloy. *J Alloys Compd* [Internet]. 2013;578:454–64. Available from: <http://dx.doi.org/10.1016/j.jallcom.2013.06.045>
- [5] Attallah MM, Jennings R, Wang X, Carter LN. Additive manufacturing of Ni-based superalloys: The outstanding issues. *MRS Bull.* 2016;41(10):758–64.
- [6] Safari J, Nategh S. On the heat treatment of Rene-80 nickel-base superalloy. *J Mater Process Technol.* 2006;176(1–3):240–50.

[TORNA ALL'INDICE >](#)